Biochemistry and Biophysics Reports 3 (2015) 51–61

Contents lists available at ScienceDirect

Biochemistry and Biophysics Reports

journal homepage: www.elsevier.com/locate/bbrep

Transcriptome-based reconstructions from the murine knockout suggest involvement of the urate transporter, URAT1 (slc22a12), in novel metabolic pathways

Satish A. Eraly [a,*], Henry C. Liu [a], Neema Jamshidi [b], Sanjay K. Nigam [a,c,d]

[a] Department of Medicine, University of California, San Diego, La Jolla, CA 92093
[b] Department of Radiology, University of California, Los Angeles, Los Angeles, CA 90095
[c] Department of Pediatrics, University of California, San Diego, La Jolla, CA 92093
[d] Department of Cellular and Molecular Medicine, University of California, San Diego, La Jolla, CA 92093

ARTICLE INFO

Article history:
Received 25 May 2015
Received in revised form
13 July 2015
Accepted 20 July 2015
Available online 21 July 2015

Keywords:
Metabolic networks
Transcriptomics
Organic anion transporter
URAT1 (slc22a12)
Urate

ABSTRACT

URAT1 (slc22a12) was identified as the transporter responsible for renal reabsorption of the medically important compound, uric acid. However, subsequent studies have indicated that other transporters make contributions to this process, and that URAT1 transports other organic anions besides urate (including several in common with the closely related multi-specific renal organic anion transporters, OAT1 (slc22a6) and OAT3 (slc22a8)). These findings raise the possibility that urate transport is not the sole physiological function of URAT1. We previously characterized mice null for the murine ortholog of URAT1 (mURAT1; previously cloned as RST), finding a relatively modest decrement in urate reabsorptive capacity. Nevertheless, there were shifts in the plasma and urinary concentrations of multiple small molecules, suggesting significant metabolic changes in the knockouts. Although these molecules remain unidentified, here we have computationally delineated the biochemical networks consistent with transcriptomic data from the null mice. These analyses suggest alterations in the handling of not only urate but also other putative URAT1 substrates comprising intermediates in nucleotide, carbohydrate, and steroid metabolism. Moreover, the analyses indicate changes in multiple other pathways, including those relating to the metabolism of glycosaminoglycans, methionine, and coenzyme A, possibly reflecting downstream effects of URAT1 loss. Taken together with the available substrate and metabolomic data for the other OATs, our findings suggest that the transport and biochemical functions of URAT1 overlap those of OAT1 and OAT3, and could contribute to our understanding of the relationship between uric acid and the various metabolic disorders to which it has been linked.

1. Introduction

The renal transporter, URAT1 [1], encoded by the human ortholog of the previously identified mouse gene, *RST*[2], was identified as the principal agent of proximal tubular reabsorption of uric acid, a medically important metabolite linked to renal and cardiovascular dysfunction as well as gout [3–5]. However, recent biochemical as well as genetic evidence indicates that several other transporters, including, prominently, GLUT9 [6–9], as well as ABCG2, NPT1, NPT4, and MRP4, make major contributions to the renal handling of urate (reviewed in [10–12]). Moreover, URAT1 transports not only urate, but also multiple other compounds (including endogenous metabolites such as acetoacetate, lactate, and orotate), a number of which are also substrates of the closely related multispecific renal organic anion transporters, OAT1 and OAT3 [13,14]; additionally, URAT1, like OAT1 and OAT3, is an exchanger that can mediate the bidirectional transport of its substrates [1,15]. Collectively, these findings raise the possibility that URAT1 might have significant functions distinct from urate reabsorption.

RST was established as the murine homolog of URAT1, mURAT1, on the basis of sequence homology [14,16] and functional similarity [15]. We characterized mice null for mURAT1, finding, consisted with the studies noted above, a relatively modest loss of urate reabsorptive capacity [17]. We subsequently performed metabolomic analyses of plasma and urine in these knockouts. Targeted measurements of the most abundant small organic anions did not reveal any differences between wild-type and mURAT1 knockout mice. However, global (untargeted) metabolomic measurements revealed significant changes in the plasma and

Abbreviations: OAT, organic anion transporter; CV, coefficient of variation

* Corresponding author. Fax: +858 822 3483.
E-mail address: seraly@ucsd.edu (S.A. Eraly).

http://dx.doi.org/10.1016/j.bbrep.2015.07.012

urine concentrations of multiple unknown small molecules, suggesting an altered metabolite profile in the knockouts [17].

Although the latter molecules have not yet been identified, here we have computationally defined the biochemical networks consistent with transcriptomic data from the null mice.. Computational reconstruction of metabolic networks based on the constraints imposed by extant patterns of gene expression have been demonstrated to have predictive value in a variety of model systems (reviewed in [18]). We previously implemented such approaches to identify metabolic networks associated with OAT1 and its near paralog, OAT3, via analyses of the corresponding knockout mice. These studies implicated OAT function in multiple metabolic pathways, including the pentose phosphate shunt, the Krebs cycle, and the polyamine pathway (OAT1; [18]), xenobiotic hydroxylation and glucuronidation, the metabolism of flavonoids and other products of the gut microbiome, and prostaglandin, cyclic nucleotide, and glycosaminoglycan metabolism (OAT3; [19]), findings generally consistent with the transport and metabolomic data for OAT1 and OAT3. In order to better understand the role of URAT1 beyond urate transport, we have now performed analogous global metabolic reconstructions based on transcriptomic data from mURAT1 knockout mice. Our findings suggest the involvement of mURAT1 in metabolic processes overlapping those associated with OAT1 and OAT3, including pathways relating to carbohydrate, nucleotide, glycosaminoglycan, and coenzyme A metabolism, among others.

2. Materials and METHODS

2.1. Gene expression determinations

The generation and breeding of mURAT1 knockout mice and the collection of microarray data on renal gene expression in mUrat1 and the corresponding wild-type mice was previously reported (Eraly⁎ et al., 2008). In brief, *RST*-null mice were generated by homologous recombination and then back-crossed to C57BL/6 J mice for seven generations to yield the progenitors from which experimental animals (wild-type as well as knockout) were descended. Quantitative PCR analysis of the expression of mOat1, mOat3, and mUrat1 was performed as follows: RNA from wild-type and mUrat1 knockout kidneys (n=3 per group) was purified on RNeasy columns (Qiagen, Valencia, CA), reverse transcribed using SuperScript III (Invitrogen, Carlsbad, CA), and the resulting cDNA samples was subjected to duplicate real-time PCR reactions at the University of California, San Diego/Veterans Affairs Medical Center's (UCSD/VAMC) Center for AIDS Research Genomics Core laboratory. Gene expression values were normalized to that of GAPDH in the corresponding cDNA samples. Gene-specific primer sequences (5′ to 3′) were as follows [please note that the first 18 bases (ACT GAA CCT GAC CGT ACA) on each forward primer correspond to the "Z sequence" that is complementary to the "uni-primer" used in the Amplifluor system]: mOat1 (mSlc22a6), ACT GAA CCT GAC CGT ACA GCA TGA CTG CCG AGT TCT ACC (forward) and CAG CGC CGA AGA TGA AGA G (reverse); mOat3 (mSlc22a8), ACT GAA CCT GAC CGT ACA GCA GCC CTT CAT CCC TAA TG (forward) and CCT CCC AGT AGA GTC ATG GTC AC (reverse); and mUrat1 (mSlc22a12), ACT GAA CCT GAC CGT ACA CCA TGC TAG GGC CTT TGG TA (forward) and GCA TCC AGG AGC CAT AGA CAC (reverse).

2.2. Determination of enriched functions in differentially expressed or variable genes

Renal gene expression patterns in wild-type and mURAT1 knockout mice as determined by microarray analysis were compared using VAMPIRE (http://genome.ucsd.edu/microarray; accessed February 11th, 2015), which takes variability differences between genotypes (which can be substantial (Eraly, 2014)) into account in determining the statistical significance of any gene expression differences (Hsiao et al., 2005, Hsiao et al., 2004). Differentially expressed genes were identified as those meeting the statistical significance threshold of $p < 0.05$ following Bonferroni correction for multiple comparisons. Functional annotations enriched among differentially expressed genes were determined using the AmiGO tool (http://amigo1.geneontology.org/; accessed February 11th, 2015), with the p value threshold set at 10-5 and the background set drawn from the Mouse Genome Informatics database (http://informatics.jax.org; accessed February 11th, 2015).

There appear to be, generally, highly significant differences between knockout and wild-type mice in mean gene expression variability (Eraly, 2014). Specifically, in each of multiple microarray comparisons of gene expression in wild-type and diverse knockout mice, the mean log coefficient of variation (CV) ratio (the mean, for the various measured genes, of the logs of the ratios of CV of expression in knockout to CV in wild-type – equivalent to calculating the geometric mean of the CV ratio; please see (Eraly, 2014) for the rationale for this procedure) was found to typically deviate highly significantly from zero, the expected value if there were no differences between knockout and wild-type mice in gene expression variability. Moreover, the distribution of the log CV ratios was found to be approximately Gaussian. As such, in the current study, we considered genes to be differentially variable if they fell within the top or bottom 1% of the expected distribution of the log CV ratios; i.e., had variability differences significantly greater or lesser than the mean variability difference between mURAT1 knockout and wild-type mice. Functional annotations enriched among these differentially variable genes were also determined using AmiGO, as described above for differentially expressed genes.

2.3. Gene expression-based metabolic network reconstruction

Microarray gene expression detection p-values were mapped to their corresponding reactions in the genome scale computational metabolic reconstruction, iMM1415 ((Sigurdsson et al., 2010), the murine version of the previously developed human metabolic reconstruction, Recon1 (Duarte et al., 2007)), based on gene-protein-reaction associations (Thiele and Palsson, 2010). The Gene Inactivity Moderated by Metabolism and Expression algorithm (GIMME; (Becker and Palsson, 2008)) provides summations of the most probable network flux states consistent with actively expressed genes and capable of achieving defined objective functions, thereby permitting quantification of the consistency of gene expression data with various metabolic objectives. In this study biomass was defined as the objective function, and the GIMME algorithm was used to generate the metabolic reconstructions most consistent with the wild-type and mURAT1 knockout mouse gene expression data, as previously described (Wu et al., 2013). Renal-specific uptake and secretion exchange constraints (as previously used to analyze blood pressure regulation (Chang et al., 2010)) were used across all conditions, so that calculated differences were only a function of changes in gene expression profiles. Each network reaction was then set as a required metabolic objective and the range of achievable flux states, hereafter referred to as flux-span, was calculated, providing a measure of the likelihood that the corresponding reaction was functional. Reactions having flux-span increased or decreased by two fold or greater in the mURAT1 knockout relative to wild-type mice were determined, and the proportions of these increased or decreased reactions within each of the various metabolic sub-systems of iMM1415 were calculated.

3. Results

3.1. Functional annotations enriched among genes differentially expressed or variable in the mURAT1 knockout

We previously analyzed renal gene expression in mURAT1 knockout mice [17] focusing on genes known at that time to be involved in urate metabolism and transport (including XDH, xanthine dehydrogenase; HGPRT, hypoxanthine guanine phosphoribosyl transferase; ADA, adenosine deaminase; AMPD2, adenosine monophosphate deaminase 2; PNP, purine nucleoside phosphorylase; UAT, urate transporter (galectin 9); MRP2 & 4, multidrug resistance proteins 2 & 4 (ATP-Binding Cassette Sub-Family C Members 2 & 4); NPT1, sodium-phosphate transport protein 1 (slc17a1); OAT1 and OAT3), and found no substantial changes in expression level. Examination of genes discovered since that prior report to contribute to the renal handling of urate (including glucose transporter type 9 (GLUT9; slc2a9), ATP-binding cassette, sub-family G, member 2 (ABCG2), organic anion transporter 10 (OAT10; organic cation transporter like 3; slc22a13), and sodium-phosphate transport protein 4 (NPT4; slc17a3); reviewed in [10–12]) also did not reveal any significant changes (Fig. 1A). (Note that while organic anion transporter 4 (OAT4; slc22a11) has also been implicated in renal urate transport, the murine genome appears to lack an ortholog for this transporter ([20].) Moreover, there was no significant difference between wild-type and mURAT1 knockout mice in the renal expression of the mURAT1-related transporters, OAT1 and OAT3, as determined by quantitative PCR (Fig. 1B).

However, there was differential expression in mURAT1 knockout mouse kidneys of genes involved in various aspects of metabolism, biosynthesis, cell cycle progression, apoptosis, and development, among other processes (Supplementary Table 1, [17]). Now that several studies have indicated that other proteins may be equally if not more important uric acid transporters than URAT1, and because a number of other URAT1 substrates have been identified, we used, as a first step, the gene ontology analysis tool AmiGO (http://amigo1.geneontology.org/; accessed February 11th, 2015) to quantify the enrichment of general functional annotations among the differentially expressed genes. We found the greatest enrichment to be for the terms “cellular metabolic process” ($p=3.26\times10^{-11}$) and “organic substance metabolic process” ($p=1.03\times10^{-9}$) (Fig. 2A).

We also employed an additional method based on recent data suggesting that differences in gene expression variability may contribute to phenotype independent of any changes in average gene expression (reviewed in [21]): we identified genes having significantly greater or lesser variability in the knockout compared to the wild-type – essentially, those at the extremes of the distribution of the gene by gene ratios of the coefficient of variation (CV) in knockout to CV in wild-type (please see the Methods). As with the differentially expressed genes, the differentially variable genes encompassed diverse functions, including those related to metabolism, cell cycle progression, growth factor signaling, and transcriptional regulation (Supplementary Table 2). Again as with the differentially expressed genes, though, the most significant enrichment was noted for the term “cellular metabolic process” ($p=5.48\times10^{-12}$) (Fig. 2B), providing additional support for the existence of metabolic alterations in the mURAT1 knockout, and thus for a consequential role for mURAT1 in cellular metabolism.

3.2. Comparison of metabolic reconstructions derived from wild-type and mURAT1 knockout renal transcriptomes

In order to obtain a finer-grained picture of the metabolic changes induced by deletion of mURAT1, we computationally defined the biochemical networks consistent with the transcriptomic

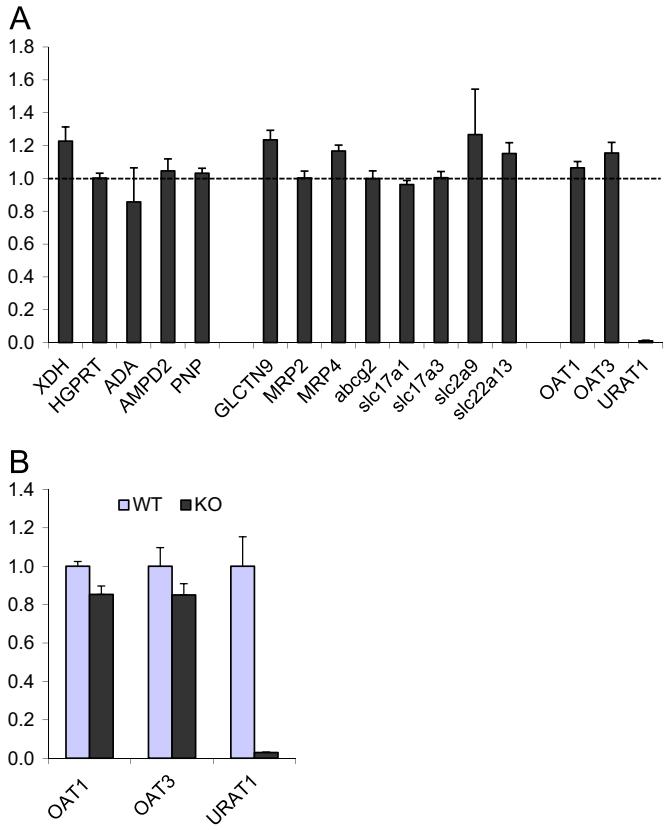

Fig. 1. Expression in mURAT1 knockout mouse kidneys of urate-regulating genes. Gene expression levels in mURAT1 knockout (KO) and wild-type (WT) mice were determined using microarrays (A) or quantitative PCR (B) and were normalized for each gene to the mean level of expression in the WT. XDH, xanthine dehydrogenase; HGPRT, hypoxanthine guanine phosphoribosyl transferase; ADA, adenosine deaminase; AMPD2, adenosine monophosphate deaminase 2; PNP, purine nucleoside phosphorylase; UAT, urate transporter (galectin 9); MRP2, multidrug resistance protein 2 (ATP-Binding Cassette Sub-Family C Member 2); MRP4, multidrug resistance protein 4 (ATP-Binding Cassette, Sub-Family C, Member 4); ABCG2, ATP-binding cassette, sub-family G, member 2; NPT1, sodium-phosphate transport protein 1 (slc17a1); NPT4, sodium-phosphate transport protein 4 (slc17a3); GLUT9, glucose transporter type 9 (slc2a9); OAT10, organic anion transporter 10 (organic cation transporter like 3; slc22a13); OAT1, organic anion transporter 1 (slc22a6); OAT3, organic anion transporter 3 (slc22a8). Data in Panel A for XDH, HGPRT, ADA, AMPD2, PNP, UAT, MRP2, MRP4, NPT1, OAT1, OAT3, and mURAT1 were reported previously [17]. Values represent mean ± standard error.

data from the knockout mice. Specifically, we assembled and analyzed murine-specific biochemical network reconstructions based on global (microarray-derived transcriptomic) renal gene expression profiles in mURAT1 knockout and wild-type mice. Gene expression data were used as weighting constraints on network reactions, and the metabolite flux-spans, which may be considered to be measures of reaction functionality, were calculated for the various reactions as previously described ([18,19]; please also see Methods). Of the ~3400 reactions in the genome scale metabolic network, iMM1415 (please see Methods), 448 (13.18%) manifested some degree of alteration in the knockout compared to wild-type reconstructions (Supplementary Table 3). Among these, 102 had flux-spans increased by greater than two fold in the knockout relative to the wild-type (Table 1), and 12 had flux-spans decreased by greater than two fold (Table 2).

The proportions of these increased and decreased reactions in the various metabolic subsystems of the reconstructions were then determined (Fig. 3). (As an example, the chondroitin sulfate metabolism subsystem comprises 44 reactions, the flux-spans of 38 of which were increased by greater than two fold in the knockout compared to the wild-type, corresponding to a

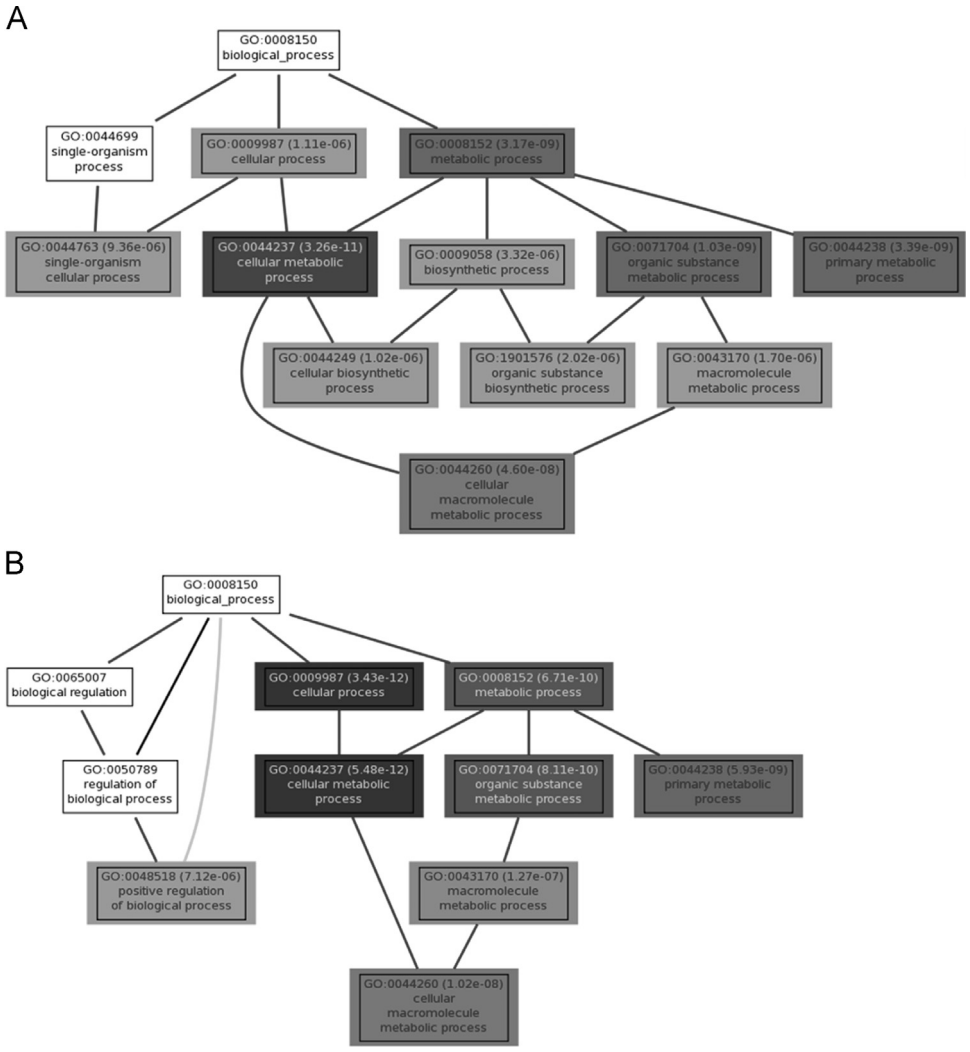

Fig. 2. Gene ontology functional annotation enrichment among genes differentially expressed or variable in the mURAT1 knockout. The enrichment of gene ontology (GO) functional annotation terms among genes that are differentially expressed (panel A) or differentially variable (panel B) in the mURAT1 knockout compared with wild-type mice was determined using AmiGO. GO terms are depicted in boxes shaded according to the statistical significance of their enrichment and p values $< 10^{-5}$ are indicated.

proportion of 0.86; Table 1 and Fig. 3A.) This analysis suggested significant increases in the mURAT1 knockout in metabolic functions related to glycosaminoglycan metabolism (aminosugar metabolism and chondroitin and keratan sulfate degradation), methionine metabolism, and lysosomal and extracellular transport (as indicated by a significant proportion of the reactions in these reconstructed sub-systems manifesting two fold or greater increase in flux-span in the knockout relative to wild-type; Table 1 and Fig. 3A). Conversely, the metabolic reconstructions featured significant decreases in functions related to coenzyme A biosynthesis (Table 2 and Fig. 3B).

Since mURAT1 is an extracellular membrane transporter, we also examined all extracellular transport reactions altered to any degree in the knockout reconstructions (and not just those having greater than two fold flux-span increases or decreases). There were 46 extracellular transport reactions, corresponding to 40 transported metabolites, having flux-span increases in the mURAT1 knockout relative to wild-type reconstructions (Table 3), and 3 reactions, corresponding to 3 metabolites, having flux-span decreases (Table 4). About a third of the compounds overall comprise small organic anions of the kind that typically (although not exclusively [18,19,22,23]) comprise substrates and inhibitors of the multispecific OATs (Tables 3 and 4). Alterations in the reconstructions of transport of the remaining compounds might reflect downstream consequences of the loss of URAT1.

In vitro data on the interactions of endogenous substrates with URAT1 provide experimental support for these analyses. Four of the compounds manifesting altered transport in the reconstructions have been demonstrated to interact with URAT1 *in vitro*; these comprise urate as well as 2-oxoglutarate (α-ketoglutarate), acetoacetate, and lactate [13]. Another two – pyruvate and progesterone – are known to interact with other members of the organic anion transporter (OAT) family of which URAT1 is a member [13,14,23]. Notably, nearly half (four of ten) of the URAT1-interacting compounds of endogenous origin that were listed in a comprehensive review [13] manifested altered transport in the knockout reconstructions (Table 5), supporting the validity of our analyses.

4. Discussion

Multiple lines of evidence indicate an important role for URAT1 in the renal reabsorption of urate; in particular loss of function URAT1 mutations have been repeatedly associated with decreased urate reabsorption, resulting in hypouricemia, exercise-induced

Table 1
Reactions having greater than two fold-increased flux-span in the mURAT1 knockout relative to wild-type reconstructions. Reactions are sorted by metabolic subsystem and then by flux-span ratio. The key to the abbreviations for reactions and formulae is available at the Biochemically, Genetically and Genomically structured genome-scale metabolic network reconstructions database (BiGG; http://bigg.ucsd.edu/bigg/; accessed February 11th, 2015). KO, mURAT1 knockout; WT, wild-type.

Reaction	Subsystem	Formula	WT Flux-span	KO Flux-span	Ratio (KO/WT)
CMPSAS	Aminosugar Metabolism	acnam(c)+ctp(c) -> cmpacna(c)+ppi(c)	0.00	2.00	Inf
CMPSASn	Aminosugar Metabolism	acnam(n)+ctp(n) -> cmpacna(n)+ppi(n)	0.00	2.00	Inf
ACGALK	Aminosugar Metabolism	acgal(c)+atp(c) -> acgal1p(c)+adp(c)+h(c)	0.00	6.50	Inf
ACGALK2	Aminosugar Metabolism	acgal(c)+itp(c) -> acgal1p(c)+h(c)+idp(c)	0.00	6.50	Inf
UAGALDP	Aminosugar Metabolism	acgal1p(c)+h(c)+utp(c) -> ppi(c)+udpacgal(c)	0.00	6.50	Inf
NACHEX5ly	Chondroitin sulfate degradation	cs_c_deg4(l)+h2o(l) -> acgal(l)+cs_c_deg5(l)	0.00	1.00	Inf
CSAPASEly	Chondroitin sulfate degradation	cspg_a(l)+h2o(l) -> Ser-Gly/Ala-X-Gly(l)+cs_a(l)	0.00	1.00	Inf
CSCPASEly	Chondroitin sulfate degradation	cspg_c(l)+h2o(l) -> Ser-Gly/Ala-X-Gly(l)+cs_c(l)	0.00	1.00	Inf
CSDPASEly	Chondroitin sulfate degradation	cspg_d(l)+h2o(l) -> Ser-Gly/Ala-X-Gly(l)+cs_d(l)	0.00	1.00	Inf
CSEPASEly	Chondroitin sulfate degradation	cspg_e(l)+h2o(l) -> Ser-Gly/Ala-X-Gly(l)+cs_e(l)	0.00	1.00	Inf
GLCAASE4ly	Chondroitin sulfate degradation	cs_a_deg2(l)+h2o(l) -> cs_a_deg3(l)+glcur(l)	0.00	1.00	Inf
GLCAASE5ly	Chondroitin sulfate degradation	cs_c_deg2(l)+h2o(l) -> cs_c_deg3(l)+glcur(l)	0.00	1.00	Inf
GLCAASE6ly	Chondroitin sulfate degradation	cs_d_deg3(l)+h2o(l) -> cs_d_deg4(l)+glcur(l)	0.00	1.00	Inf
GLCAASE7ly	Chondroitin sulfate degradation	cs_e_deg3(l)+h2o(l) -> cs_e_deg4(l)+glcur(l)	0.00	1.00	Inf
LINKDEG2ly	Chondroitin sulfate degradation	cs_a_deg5(l)+4 h2o(l) -> 2 gal(l)+glcur(l)+h(l)+so4(l)+xyl-D(l)	0.00	1.00	Inf
LINKDEG4ly	Chondroitin sulfate degradation	cs_e_deg7(l)+5 h2o(l) -> 2 gal(l)+glcur(l)+2 h(l)+2 so4(l)+xyl-D(l)	0.00	1.00	Inf
NACHEX1ly	Chondroitin sulfate degradation	cs_a_deg1(l)+h2o(l) -> acgal(l)+cs_a_deg2(l)	0.00	1.00	Inf
NACHEX2ly	Chondroitin sulfate degradation	cs_a_deg4(l)+h2o(l) -> acgal(l)+cs_a_deg5(l)	0.00	1.00	Inf
NACHEX4ly	Chondroitin sulfate degradation	cs_c_deg1(l)+h2o(l) -> acgal(l)+cs_c_deg2(l)	0.00	1.00	Inf
NACHEX6ly	Chondroitin sulfate degradation	cs_d_deg1(l)+h2o(l) -> acgal(l)+cs_d_deg2(l)	0.00	1.00	Inf
NACHEX7ly	Chondroitin sulfate degradation	cs_d_deg5(l)+h2o(l) -> acgal(l)+cs_d_deg6(l)	0.00	1.00	Inf
NACHEX8ly	Chondroitin sulfate degradation	cs_e_deg2(l)+h2o(l) -> acgal(l)+cs_e_deg3(l)	0.00	1.00	Inf
NACHEX9ly	Chondroitin sulfate degradation	cs_e_deg6(l)+h2o(l) -> acgal(l)+cs_e_deg7(l)	0.00	1.00	Inf
NACHEXA1ly	Chondroitin sulfate degradation	cs_a(l)+2 h2o(l) -> acgal(l)+cs_a_deg2(l)+h(l)+so4(l)	0.00	1.00	Inf
NACHEXA3ly	Chondroitin sulfate degradation	cs_c(l)+2 h2o(l) -> acgal(l)+cs_c_deg2(l)+h(l)+so4(l)	0.00	1.00	Inf
NACHEXA4ly	Chondroitin sulfate degradation	cs_c_deg3(l)+2 h2o(l) -> acgal(l)+cs_c_deg5(l)+h(l)+so4(l)	0.00	1.00	Inf
NACHEXA5ly	Chondroitin sulfate degradation	cs_d(l)+2 h2o(l) -> acgal(l)+cs_d_deg2(l)+h(l)+so4(l)	0.00	1.00	Inf
NACHEXA6ly	Chondroitin sulfate degradation	cs_d_deg4(l)+2 h2o(l) -> acgal(l)+cs_d_deg6(l)+h(l)+so4(l)	0.00	1.00	Inf
NACHEXA7ly	Chondroitin sulfate degradation	cs_e(l)+3 h2o(l) -> acgal(l)+cs_e_deg3(l)+2 h(l)+2 so4(l)	0.00	1.00	Inf
NACHEXA8ly	Chondroitin sulfate degradation	cs_e_deg4(l)+3 h2o(l) -> acgal(l)+cs_e_deg7(l)+2 h(l)+2 so4(l)	0.00	1.00	Inf
S2TASE4ly	Chondroitin sulfate degradation	cs_d_deg2(l)+h2o(l) -> cs_d_deg3(l)+h(l)+so4(l)	0.00	1.00	Inf
S2TASE5ly	Chondroitin sulfate degradation	cs_d_deg6(l)+h2o(l) -> cs_c_deg5(l)+h(l)+so4(l)	0.00	1.00	Inf
S4TASE1ly	Chondroitin sulfate degradation	cs_a(l)+h2o(l) <=> cs_a_deg1(l)+h(l)+so4(l)	0.00	1.00	Inf
S4TASE2ly	Chondroitin sulfate degradation	cs_a_deg3(l)+h2o(l) <=> cs_a_deg4(l)+h(l)+so4(l)	0.00	1.00	Inf
S4TASE4ly	Chondroitin sulfate degradation	cs_e(l)+h2o(l) <=> cs_e_deg1(l)+h(l)+so4(l)	0.00	1.00	Inf
S4TASE5ly	Chondroitin sulfate degradation	cs_e_deg4(l)+h2o(l) <=> cs_e_deg5(l)+h(l)+so4(l)	0.00	1.00	Inf
S6TASE4ly	Chondroitin sulfate degradation	cs_c(l)+h2o(l) <=> cs_c_deg1(l)+h(l)+so4(l)	0.00	1.00	Inf
S6TASE5ly	Chondroitin sulfate degradation	cs_c_deg3(l)+h2o(l) <=> cs_c_deg4(l)+h(l)+so4(l)	0.00	1.00	Inf
S6TASE6ly	Chondroitin sulfate degradation	cs_d(l)+h2o(l) <=> cs_d_deg1(l)+h(l)+so4(l)	0.00	1.00	Inf
S6TASE7ly	Chondroitin sulfate degradation	cs_d_deg4(l)+h2o(l) <=> cs_d_deg5(l)+h(l)+so4(l)	0.00	1.00	Inf
S6TASE8ly	Chondroitin sulfate degradation	cs_e_deg1(l)+h2o(l) <=> cs_e_deg2(l)+h(l)+so4(l)	0.00	1.00	Inf
S6TASE9ly	Chondroitin sulfate degradation	cs_e_deg5(l)+h2o(l) <=> cs_e_deg6(l)+h(l)+so4(l)	0.00	1.00	Inf
LINKDEG3ly	Chondroitin sulfate degradation	cs_c_deg5(l)+4 h2o(l) -> 2 gal(l)+glcur(l)+h(l)+so4(l)+xyl-D(l)	0.00	2.00	Inf
MTHFCm	Folate Metabolism	h2o(m)+methf(m) <=> 10fthf(m)+h(m)	8.00	414.75	51.84
MTHFR3	Folate Metabolism	2 h(c)+mlthf(c)+nadph(c) -> 5mthf(c)+nadp(c)	7.00	417.73	59.68
MTHFC	Folate Metabolism	h2o(c)+methf(c) <=> 10fthf(c)+h(c)	83.00	450.59	5.43
CHOLK	Glycerophospholipid Metabolism	atp(c)+chol(c) -> adp(c)+cholp(c)+h(c)	412.86	1000.00	2.42
ETHAK	Glycerophospholipid Metabolism	atp(c)+etha(c) -> adp(c)+ethamp(c)+h(c)	412.86	1000.00	2.42
GNMT	Glycine, Serine, and Threonine Metabolism	amet(c)+gly(c) -> ahcys(c)+h(c)+sarcs(c)	4.00	412.86	103.22
GALASE16ly	Keratan sulfate degradation	2 h2o(l)+ksii_core2_deg2(l) -> 2 gal(l)+ksii_core2_deg3(l)	0.00	1.00	Inf
GALASE20ly	Keratan sulfate degradation	2 h2o(l)+ksii_core4_deg2(l) -> 2 gal(l)+ksii_core4_deg3(l)	0.00	1.00	Inf
NACHEX23ly	Keratan sulfate degradation	h2o(l)+ksii_core2_deg4(l) -> acgam(l)+ksii_core2_deg5(l)	0.00	1.00	Inf
NACHEX26ly	Keratan sulfate degradation	2 h2o(l)+ksii_core4_deg4(l) -> 2 acgam(l)+ksii_core2_deg5(l)	0.00	1.00	Inf
NACHEXA20ly	Keratan sulfate degradation	2 h2o(l)+ksii_core2_deg3(l) -> acgam(l)+h(l)+ksii_core2_deg5(l)+so4(l)	0.00	1.00	Inf
NACHEXA22ly	Keratan sulfate degradation	3 h2o(l)+ksii_core4_deg3(l) -> 2 acgam(l)+h(l)+ksii_core2_deg5(l)+so4(l)	0.00	1.00	Inf
S6TASE22ly	Keratan sulfate degradation	h2o(l)+ksii_core2_deg1(l) <=> h(l)+ksii_core2_deg2(l)+so4(l)	0.00	1.00	Inf
S6TASE23ly	Keratan sulfate degradation	h2o(l)+ksii_core2_deg3(l) <=> h(l)+ksii_core2_deg4	0.00	1.00	Inf

Table 1 (*continued*)

Reaction	Subsystem	Formula	WT Flux-span	KO Flux-span	Ratio (KO/WT)
		(l)+so4(l)			
S6TASE25ly	Keratan sulfate degradation	h2o(l)+ksii_core4_deg1(l) <=> h(l)+ksii_core4_deg2(l)+so4(l)	0.00	1.00	Inf
S6TASE26ly	Keratan sulfate degradation	h2o(l)+ksii_core4_deg3(l) <=> h(l)+ksii_core4_deg4(l)+so4(l)	0.00	1.00	Inf
SIAASE3ly	Keratan sulfate degradation	h2o(l)+ksii_core2(l) -> acnam(l)+ksii_core2_deg1(l)	0.00	1.00	Inf
SIAASE4ly	Keratan sulfate degradation	h2o(l)+ksii_core4(l) -> acnam(l)+ksii_core4_deg1(l)	0.00	1.00	Inf
GALASE17ly	Keratan sulfate degradation	h2o(l)+ksii_core2_deg5(l) -> gal(l)+ksii_core2_deg6(l)	0.00	2.00	Inf
GALASE18ly	Keratan sulfate degradation	h2o(l)+ksii_core2_deg8(l) -> gal(l)+ksii_core2_deg9(l)	0.00	2.00	Inf
GALASE19ly	Keratan sulfate degradation	f1a(l)+h2o(l) -> core6(l)+gal(l)	0.00	2.00	Inf
NACHEX24ly	Keratan sulfate degradation	h2o(l)+ksii_core2_deg7(l) -> acgam(l)+ksii_core2_deg8(l)	0.00	2.00	Inf
NACHEX25ly	Keratan sulfate degradation	h2o(l)+ksii_core2_deg9(l) -> acgam(l)+f1a(l)	0.00	2.00	Inf
NACHEXA21ly	Keratan sulfate degradation	2 h2o(l)+ksii_core2_deg6(l) -> acgam(l)+h(l)+ksii_core2_deg8(l)+so4(l)	0.00	2.00	Inf
NAGA2ly	Keratan sulfate degradation	Tn_antigen(l)+h(l)+udp(l) -> Ser/Thr(l)+udpacgal(l)	0.00	2.00	Inf
NAGLCAly	Keratan sulfate degradation	core6(l)+h2o(l) -> Tn_antigen(l)+acgam(l)	0.00	2.00	Inf
S6TASE24ly	Keratan sulfate degradation	h2o(l)+ksii_core2_deg6(l) <=> h(l)+ksii_core2_deg7(l)+so4(l)	0.00	2.00	Inf
METAT	Methionine Metabolism	atp(c)+h2o(c)+met-L(c) -> amet(c)+pi(c)+ppi(c)	67.50	413.06	6.12
AHC	Methionine Metabolism	ahcys(c)+h2o(c) <=> adn(c)+hcys-L(c)	4.00	413.06	103.27
PUNP1	Nucleotides	adn(c)+pi(c) <=> ade(c)+r1p(c)	312.00	684.67	2.19
6HTSTSTERONEtr	Transport, Endoplasmic Reticular	6htststerone(c) <=> 6htststerone(r)	0.00	1.00	Inf
6HTSTSTERONEte	Transport, Extracellular	6htststerone(c) <=> 6htststerone(e)	0.00	1.00	Inf
AFLATOXINte	Transport, Extracellular	aflatoxin(e) <=> aflatoxin(c)	0.00	1.00	Inf
EAFLATOXINte	Transport, Extracellular	eaflatoxin(e) <=> eaflatoxin(c)	0.00	1.00	Inf
XYLt	Transport, Extracellular	xyl-D(e) <=> xyl-D(c)	0.00	3.25	Inf
CAATPS	Transport, Extracellular	atp(c)+2 ca2(c)+h2o(c) -> adp(c)+pi(c)+2 ca2(e)+h(e)	500.00	1000.00	2.00
CAt7r	Transport, Extracellular	ca2(c)+3 na1(e) <=> 3 na1(c)+ca2(e)	1000.00	2000.00	2.00
NRPPHRtu	Transport, Extracellular	nrpphr(e) <=> nrpphr(c)	1000.00	2000.00	2.00
CMPACNAtg	Transport, Golgi Apparatus	cmpacna(c)+cmp(g) <=> cmp(c)+cmpacna(g)	0.00	2.00	Inf
CSPG_Atly	Transport, Lysosomal	cspg_a(e) -> cspg_a(l)	0.00	1.00	Inf
CSPG_Ctly	Transport, Lysosomal	cspg_c(e) -> cspg_c(l)	0.00	1.00	Inf
CSPG_Dtly	Transport, Lysosomal	cspg_d(e) -> cspg_d(l)	0.00	1.00	Inf
CSPG_Etly	Transport, Lysosomal	cspg_e(e) -> cspg_e(l)	0.00	1.00	Inf
KSII_CORE2tly	Transport, Lysosomal	ksii_core2(e) -> ksii_core2(l)	0.00	1.00	Inf
KSII_CORE4tly	Transport, Lysosomal	ksii_core4(e) -> ksii_core4(l)	0.00	1.00	Inf
UDPACGALtl	Transport, Lysosomal	udpacgal(c) <=> udpacgal(l)	0.00	2.00	Inf
UDPtl	Transport, Lysosomal	udp(c) <=> udp(l)	0.00	2.00	Inf
XYLtly	Transport, Lysosomal	xyl-D(l) -> xyl-D(c)	0.00	3.25	Inf
ACGALtly	Transport, Lysosomal	acgal(l) -> acgal(c)	0.00	6.50	Inf
GLCURtly	Transport, Lysosomal	glcur(c)+h(c) <=> glcur(l)+h(l)	2.00	8.50	4.25
SO4tl	Transport, Lysosomal	so4(l) <=> so4(c)	6.00	15.33	2.56
GALtly	Transport, Lysosomal	gal(l) -> gal(c)	4.00	19.33	4.83
SARCStm	Transport, Mitochondrial	sarcs(c) -> sarcs(m)	5.00	413.77	82.75
GLYtm	Transport, Mitochondrial	gly(c) <=> gly(m)	9.00	415.17	46.13
10FTHFtm	Transport, Mitochondrial	10fthf(c) <=> 10fthf(m)	324.50	666.67	2.05
ACNAMtn	Transport, Nuclear	acnam(c) -> acnam(n)	0.00	2.00	Inf
CMPACNAtn	Transport, Nuclear	cmpacna(n) -> cmpacna(c)	0.00	2.00	Inf
CTPtn	Transport, Nuclear	ctp(c) <=> ctp(n)	0.00	2.00	Inf
SARDHm	Urea cycle/amino group metabolism	fad(m)+sarcs(m)+thf(m) -> fadh2(m)+gly(m)+mlthf(m)	8.00	414.75	51.84

Table 2
Reactions having greater than two fold-decreased flux-span in the mURAT1 knockout relative to wild-type reconstructions. Reactions are sorted by metabolic subsystem and then by flux-span ratio. The key to the abbreviations for reactions and formulae is available at the Biochemically, Genetically and Genomically structured genome-scale metabolic network reconstructions database (BiGG; http://bigg.ucsd.edu/bigg/; accessed February 11th, 2015). KO, mURAT1 knockout; WT, wild-type.

Reaction	Subsystem	Formula	WT Flux-span	KO Flux-span	Ratio (KO/WT)
DPCOAK	CoA Biosynthesis	atp(c)+dpcoa(c) -> adp(c)+coa(c)+h(c)	1.00	0.00	0.00
PNTK	CoA Biosynthesis	atp(c)+pnto-R(c) -> 4ppan(c)+adp(c)+h(c)	1.00	0.00	0.00
PPCDC	CoA Biosynthesis	4ppcys(c)+h(c) -> co2(c)+pan4p(c)	1.00	0.00	0.00
PPNCL3	CoA Biosynthesis	4ppan(c)+atp(c)+cys-L(c) -> 4ppcys(c)+amp(c)+h(c)+ppi(c)	1.00	0.00	0.00
HSD3B11	Steroid Metabolism	nad(c)+prgnlone(c) -> h(c)+nadh(c)+prgstrn(c)	1.00	0.00	0.00
AKR1C1	Steroid Metabolism	h(c)+nadph(c)+prgstrn(c) -> aprgstrn(c)+nadp(c)	2.00	1.00	0.50
4MPTNLte	Transport, Extracellular	4mptnl(c) <=> 4mptnl(e)	1.00	0.00	0.00
APRGSTRNte	Transport, Extracellular	aprgstrn(e) <=> aprgstrn(c)	2.00	1.00	0.50
PRGSTRNt	Transport, Extracellular	prgstrn(e) <=> prgstrn(c)	2.00	1.00	0.50
4MPTNLtm	Transport, Mitochondrial	4mptnl(c) <=> 4mptnl(m)	1.00	0.00	0.00
PRGNLONEtm	Transport, Mitochondrial	prgnlone(c) <=> prgnlone(m)	1.00	0.00	0.00
3HLYTCL	Tyrosine metabolism	34dhphe(c)+h(c) -> co2(c)+dopa(c)	1.00	0.00	0.00

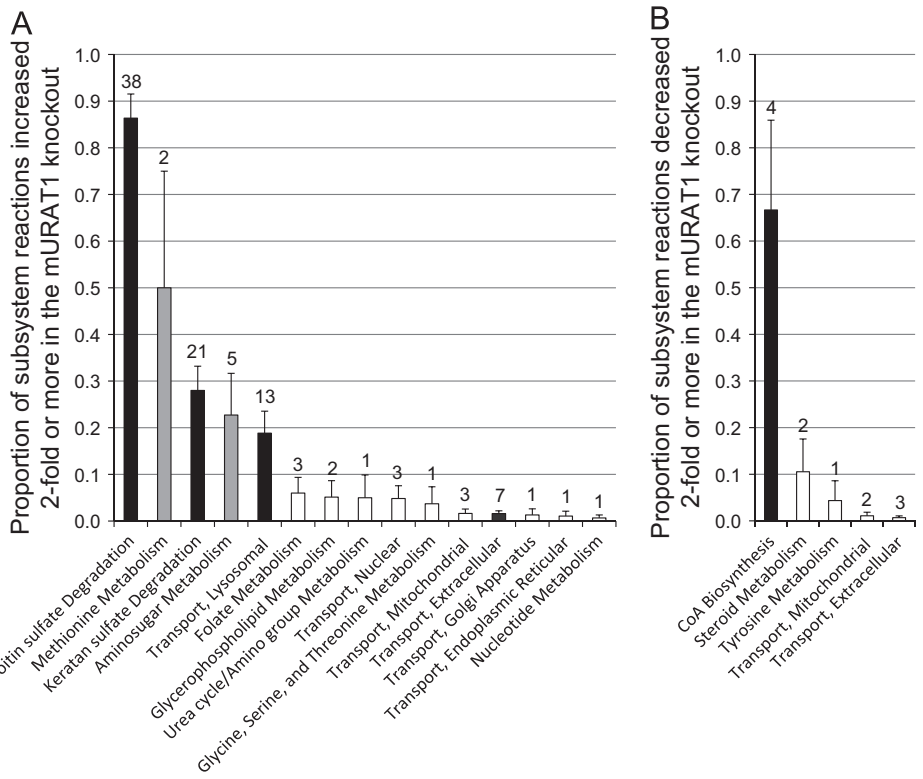

Fig. 3. Metabolic sub-systems containing reactions with two-fold or greater change in flux-span in mURAT1 knockout reconstructions. Proportions of the indicated metabolic sub-systems comprising reactions having flux-spans increased (panel A) or decreased (panel B) by two-fold or greater in the mURAT1 knockout relative to wild-type reconstructions are depicted. The actual number of reactions increased or decreased by two-fold or greater than is indicated above each column. Error bars denote the standard error of the proportion; black columns, $p < 0.001$; dark gray columns, $p < 0.01$; light gray columns, $p < 0.05$; open columns, NS.

renal failure, nephrolithiasis, and as recently demonstrated, endothelial dysfunction [24–28]. However, as noted in the Introduction, recent data indicates that other transporters also make significant contributions to urate reabsorption [11,17,29,30] and that URAT1 has other substrates besides urate (Table 5). These findings suggest additional functions for URAT1 beyond urate transport. Consistent with this notion, the metabolic reconstructions presented here, based on computational definition of the biochemical pathways consistent with the mURAT1 knockout transcriptomic data, suggest multiple metabolic alterations in the mURAT1 knockout mouse distinct from urate handling. As discussed further below, the set of metabolic reactions associated with mURAT1 manifests some commonalities with those previously reported for the related transporters, OAT1 and OAT3 [18,19]. It is also notable that many more reactions had increased functionality in the mURAT1 knockout mouse reconstructions than had decreased functionality, possibly indicating that loss of mURAT1 induces a heightened state of metabolic compensation. This is in contrast to the OAT1 and OAT3 knockout reconstructions which had more reactions with decreased than increased functionality [18,19].

Metabolites having altered extracellular membrane transport in the mURAT1 knockout mouse reconstructions included several that are plausible URAT1 substrates on the basis of their previously demonstrated *in vitro* interactions with this transporter and/or other OAT family members (Tables 3 and 4) – indeed, four of the ten known URAT1-interacting substrates of endogenous origin were represented among these molecules (Table 5). Overall, these findings suggest the potential involvement of URAT1 in bioenergetic pathways (via transport of acetoacetate, α-ketoglutarate, lactate, and pyruvate), nucleotide metabolism (via transport of urate), and steroid signaling or metabolism (via transport of or interaction with progesterone). With regard to the latter process, progestgerone and two other intermediates in steroid metabolism ((20 S)-20-hydroxypregn-4-en-3-one and 4-methylpentanal) comprised the three compounds manifesting decreased transport in the knockout reconstructions (each by two fold or greater).

Alterations in the reconstructions of transport of non-OAT substrates and of the non-transport metabolic subsystems presumably reflect possible secondary or downstream effects of mURAT1 loss, including those due to genomic regulatory feedback. These changes involved multiple cellular processes and biochemical pathways taking place in the cytosol, lysosomes, and mitochondria. Prominent among them were increases in functionalities relating to lysosomal turnover of glycosaminoglycans (polymers of aminosugars that constitute the glycan component of glycosylated proteins [31,32]): A significant proportion of the reactions belonging to the subsystems of aminosugar metabolism and degradation of the glycosaminoglycans, chondroitin and keratan sulfate, had flux-span increases greater than two fold in the mURAT1 knockout compared with wild-type reconstructions (Fig. 3A). Moreover, in the lysosomal transport sub-system, which also had a significant proportion of increased reactions in the knockout reconstructions, all of the affected reactions involved transport of glycosaminoglycans or aminosugars (Fig. 3A and Table 1). Notably, altered glycosaminoglycan metabolism was also a feature of our gene expression-constrained reconstructions of metabolism in the OAT1 and OAT3 knockouts [18,19].

Glycosaminoglycans are not only important elements of the extracellular matrix but are also critical to cell-cell communication mediated by integral membrane proteins and soluble factors [32]. For example, emerging evidence indicates that extracellular matrix glycosaminoglycans may modulate growth factor signaling during branching morphogenesis in the kidney (reviewed in [33]). Thus, our findings suggesting altered metabolism of these molecules in mURAT1 knockout mice raise the possibility of a role for mURAT1

Table 3
Metabolites associated with extracellular transport reactions having increased flux-span in the mURAT1 knockout reconstructions. Metabolites are sorted by whether or not they are known to interact with URAT1 or other members of the organic anion transporter (OAT) family, and then by the flux-span ratios of their associated transport reactions. The key to the abbreviations for reactions and formulae is available at the Biochemically, Genetically and Genomically structured genome-scale metabolic network reconstructions database (BiGG; http://bigg.ucsd.edu/bigg/; accessed February 11th, 2015). KO, mURAT1 knockout; WT, wild-type; x, OAT-interacting compound; y, URAT1-interacting compound. Transporter-metabolite interactions were derived from a comprehensive review [13].

Metabolite Name	OAT-interacting compound	URAT1-interacting compound	Transport Reaction	Formula	WT Flux-span	KO Flux-span	Flux-span Ratio (KO/WT)
Urate	x	y	URATEt	urate(c) -> urate(e)	39.333	42.389	1.078
Acetoacetate	x	y	ACACt2	acac(e)+h(e) <=> acac(c)+h(c)	288.027	308.913	1.073
Lactate	x	y	D-LACt2	h(e)+lac-D(e) <=> h(c)+lac-D(c)	290.771	311.816	1.072
2-Oxoglutarate	x	y	AKGt4_3	akg(e)+3 na1(e) <=> akg(c)+3 na1(c)	149.401	159.910	1.070
Pyruvate	x		PYRt2r	h(e)+pyr(e) <=> h(c)+pyr(c)	293.212	313.866	1.070
6 beta hydroxy testosterone			6HTSTSTERONEte	6htststerone(c) <=> 6htststerone(e)	0.000	1.000	Inf
aflatoxin B1			AFLATOXINte	aflatoxin(e) <=> aflatoxin(c)	0.000	1.000	Inf
aflatoxin B1 exo-8,9-epoxide			EAFLATOXINte	eaflatoxin(e) <=> eaflatoxin(c)	0.000	1.000	Inf
D-Xylose			XYLt	xyl-D(e) <=> xyl-D(c)	0.000	3.250	Inf
Calcium			CAATPS	atp(c)+2 ca2(c)+h2o(c) -> adp(c)+pi(c)+2 ca2(e)+h(e)	500.000	1000.000	2.000
Calcium			CAt7r	ca2(c)+3 na1(e) <=> 3 na1(c)+ca2(e)	1000.000	2000.000	2.000
Norepinephrine			NRPPHRtu	nrpphr(e) <=> nrpphr(c)	1000.000	2000.000	2.000
Dopamine			DOPAtu	dopa(e) <=> dopa(c)	1001.000	2000.000	1.998
Norepinephrine			NRPPHRVESSEC	2 atp(c)+2 h2o(c)+3 nrpphr(c) -> 2 adp(c)+2 h(c)+2 pi(c)+3 nrpphr(e)	333.333	520.601	1.562
Dopamine			DOPAVESSEC	2 atp(c)+3 dopa(c)+2 h2o(c) -> 2 adp(c)+2 h(c)+2 pi(c)+3 dopa(e)	333.667	520.601	1.560
Dehydroascorbate			DHAAt1r	dhdascb(e) <=> dhdascb(c)	101.833	125.500	1.232
L-Arabinitol			ABTti	abt(c) -> abt(e)	102.167	125.833	1.232
Xylitol			XYLTt	xylt(e) <=> xylt(c)	102.167	125.833	1.232
D-Fructose			FRUt4	fru(e)+na1(e) <=> fru(c)+na1(c)	101.000	123.778	1.226
Deoxyribose			DRIBt	drib(e) <=> drib(c)	124.000	151.333	1.220
Acetaldehyde			ACALDt	acald(e) <=> acald(c)	312.000	380.333	1.219
Deoxyuridine			DURIt	duri(e) <=> duri(c)	63.500	72.667	1.144
Uridine			URIt	uri(e) <=> uri(c)	63.500	72.667	1.144
Cytidine			CYTDt	cytd(e) <=> cytd(c)	42.333	48.444	1.144
Formate			CLFORtex	2 for(c)+cl(e) -> cl(c)+2 for(e)	33.750	38.333	1.136
Glycerol			GLYCt	glyc(c) <=> glyc(e)	134.405	149.252	1.110
Methylglyoxal			MTHGXLt	mthgxl(c) -> mthgxl(e)	500.000	553.431	1.107
Guanosine			GSNt	gsn(e) <=> gsn(c)	33.714	36.333	1.078
Deoxyguanosine			DGSNt	dgsn(e) <=> dgsn(c)	33.714	36.333	1.078
Hexadecenoate (n-C16:1); Palmitoleic acid			HDCEAtr	hdcea(e) <=> hdcea(c)	92.023	98.585	1.071
linoelaidic acid (all trans C18:2)			LNELDCt	lneldc(e) <=> lneldc(c)	79.926	85.613	1.071
elaidic acid			ELAIDt	elaid(e) <=> elaid(c)	80.997	86.748	1.071
vaccenic acid			VACCt	vacc(e) <=> vacc(c)	80.997	86.748	1.071
acetone			ACETONEt2	acetone(e)+h(e) <=> acetone(c)+h(c)	463.750	494.880	1.067
fatty acid retinol			RETFAt	retfa(c) -> retfa(e)	309.429	330.167	1.067
Retinol			RETt	retinol(e) -> retinol(c)	306.658	327.167	1.067
diacylglycerol			DAGt	dag_hs(e) <=> dag_hs(c)	348.108	371.373	1.067
(R)-3-Hydroxybutanoate			BHBt	bhb(e)+h(e) <=> bhb(c)+h(c)	285.288	304.282	1.067
R total 2 position			RTOTAL2t	Rtotal2(e) <=> Rtotal2(c)	393.916	420.137	1.067
triacylglycerol			TAGt	tag_hs(e) <=> tag_hs(c)	308.684	329.194	1.066
R total 3 position			RTOTAL3t	Rtotal3(e) <=> Rtotal3(c)	396.916	423.137	1.066
monoacylglycerol 3			MAGt	mag_hs(e) <=> mag_hs(c)	78.635	83.736	1.065
R total			RTOTALt	Rtotal(e) <=> Rtotal(c)	91.250	96.970	1.063
omega hydroxy tetradecanoate (n-C14:0)			WHTTDCAte	whttdca(e) <=> whttdca(c)	92.762	95.786	1.033
omega hydroxy tetradecanoate (n-C14:0)			WHHDCAte	whhdca(e) <=> whhdca(c)	83.381	85.236	1.022
hydrogen peroxide			H2O2t	h2o2(e) <=> h2o2(c)	1158.530	1159.224	1.001

Table 4
Metabolites associated with extracellular transport reactions having decreased flux-span in the mURAT1 knockout reconstructions. Metabolites are sorted by whether or not they are known to interact with URAT1 or other members of the organic anion transporter (OAT) family, and then by the flux-span ratios of their associated transport reactions. The key to the abbreviations for reactions and formulae is available at the Biochemically, Genetically and Genomically structured genome-scale metabolic network reconstructions database (BiGG; http://bigg.ucsd.edu/bigg/; accessed February 11th, 2015). KO, mURAT1 knockout; WT, wild-type; x, OAT-interacting compound. Transporter-metabolite interactions were derived from a comprehensive review [13].

Metabolite Name	OAT-interacting compound	URAT1-interacting compound	Transport Reaction	Transport Reaction Formula	WT Flux-span	KO Flux-span	Flux-span Ratio (KO/WT)
progesterone	x		PRGSTRNt	prgstrn(e) <=> prgstrn(c)	2.000	1.000	0.500
4-methylpentanal			4MPTNLte	4mptnl(c) <=> 4mptnl(e)	1.000	0.000	0.000
(20 S)-20-hydroxypregn-4-en-3-one			APRGSTRNte	aprgstrn(e) <=> aprgstrn(c)	2.000	1.000	0.500

Table 5
Endogenous URAT1-interacting compounds from a comprehensive review [13]. Shaded rows indicate compounds manifesting altered transport in the mURAT1 knockout reconstructions. h, human; m, mouse; r, rat.

URAT1-interacting compound	URAT1 ortholog tested	Expression System
Acetoacetate	h	*X.laevis*
Dehydroepiandrosterone sulfate	m	HEK293 cell line
Hydroxybutyrate	h	*X.laevis*
Ketoglutarate	h	*X.laevis*
Lactate	h	*X.laevis*
	m	*X.laevis*
Nicotinate	h	*X.laevis*
Orotate	h	*X.laevis*
Succinate	h	*X.laevis*
Urate	h	HEK293 cell line
		X.laevis
	m	*X.laevis*
	r	Proteoliposome
β-hydroxybutyric acid	h	*X.laevis*

in renal development, though this hypothesis is somewhat mitigated by the lack of obvious developmental anomalies in the knockouts [17]. Moreover, altered glycosylation is a virtually universal feature of malignancy [32] so that URAT1 involvement in glycosaminoglycan metabolism may also have implications for pathophysiological mechanisms in cancer. Notably, glycosaminoglycans bind lipoproteins and may thereby modulate cholesterol levels [32]. Thus involvement in glycosaminoglycan metabolism may help explain the relationship between uric acid and cardiovascular disease.

Methionine and associated one-carbon metabolism also manifested increased functionality in the mURAT1 knockout reconstructions (Fig. 3A and Table 1). Methionine is a precursor to homocysteine, elevated plasma levels of which represent a cardiovascular risk factor [34]. Notably in this regard, reactions involving the metabolism of folate, which is necessary for the recycling of homocysteine to methionine and is thus cardio-protective, were also increased in the knockout reconstructions, though not to a statistically significant degree (Fig. 3A and Table 1). As with glycosaminoglycan metabolism, the possible involvement of URAT1 in methionine and folate metabolism may contribute to the links between uric acid and cardiovascular disease.

Conversely, functions related to the biosynthesis of coenzyme A, required in the Krebs cycle and for fatty acid metabolism, were significantly decreased in the mURAT1 knockout reconstructions (Fig. 3B and Table 2), consistent with the role for mURAT1 in renal cellular bioenergetics that was suggested by the alterations in the reconstructions of transport of metabolic intermediates. Of note, the URAT1-related transporters, OAT1 and OAT3, were also implicated in cellular bioenergetics in our prior network analyses [18,19]). The possible involvement of URAT1 in coenzyme A metabolism could have implications for the various neurodegenerative and metabolic disorders that involve coenzyme A dysregulation [35–37].

Accumulating data indicate that OAT1 and OAT3, previously primarily studied in terms of their role in mediating the renal secretion of numerous important organic anionic pharmaceuticals (e.g., non-steroidal anti-inflammatory drugs, β-lactam antibiotics, loop and thiazide diuretics), in fact handle a diverse array of metabolically and clinically significant endogenous substrates (e.g., Krebs cycle intermediates, uremic toxins, enterobiome products, cyclic nucleotides, prostaglandins, and steroid conjugates) [13,14,38,39], suggesting their function in various physiological processes. Indeed, mice null for OAT3 are relatively hypotensive, indicating a role for this transporter in the regulation of blood pressure [23]. Moreover, the expression of these and related transporters in widely dispersed tissues (including liver, olfactory mucosa, and choroid plexus of the brain, in addition to kidney) and their transport of signaling molecules (as listed above) raise the possibility that they participate in organism-wide communication networks (which has been termed the “remote sensing and signaling hypothesis”) [38–40]. The metabolic reconstructions presented here are in line with likewise physiological roles for mURAT1.

In summary, in the context of a growing number of URAT1 substrates other than urate, the identification of other clinically important uric acid transporters (e.g., slc2a9, ABCG2), and the presence of metabolomic changes in the mURAT1 knockout (although the involved metabolites could not be identified), we have used gene expression data from mURAT1 knockout mice to computationally constrain pathway reconstructions, thereby allowing global characterization of metabolic networks potentially associated with mURAT1. While there is need for follow up physiological studies analyzing the knockout mice under conditions of perturbed as well as basal homoeostasis, our findings suggest that mURAT1 has additional functions beyond urate reabsorption, including in bioenergtic and biosynthetic metabolism; as detailed above many of these functions overlap those of the closely related transporters, OAT1 and OAT3. Moreover, since mURAT1 and hURAT1 are at least as phylogenetically similar as most mouse-human orthologous gene pairs (they manifest 81% sequence similarity and 74% identity at the amino acid level [1,2,15], slightly superior to the mean 70.1% identity across all mouse-human orthologs [41]), these additional functions may also occur in humans. While the much higher levels of urate in humans than mice could result in greater competitive inhibition by urate of these other URAT1 functions, such inhibition would not be expected to be complete. Urate concentrations in human plasma generally fall in the range 200-500 uM, the midpoint of which, 350 μM, is approximately equivalent to the apparent affinity (K_m) of urate for URAT1, which was estimated to be 371 μM [1]. Thus, on average, circulating urate might be expected to occupy about half of the available URAT1

transporters, so that transport of any other substrates would be reduced but not eliminated. Accordingly, our findings in URAT1 knockout mice could potentially have implications for human physiology, including for our understanding of the relationship between uric acid and the various metabolic disorders to which it has been linked.

Grants

The authors acknowledge support from National Institutes of Health grants GM098449 (to SKN) and HL094728 (to SAE). The National Institutes of Health had no role in the design of the study, in the collection, analysis, and interpretation of the data; in the writing of the manuscript; and in the decision to submit the manuscript for publication.

Disclosures

The authors declare that they have no conflicts of interest.

Author contributions

SAE performed experiments, analyzed and interpreted the data, and wrote the manuscript; HCL and NJ analyzed and interpreted the data; and SKN conceived the overall research plan and interpreted the data. All authors reviewed and edited the manuscript.

Appendix A. Supplementary material

Supplementary data associated with this article can be found in the online version at http://dx.doi.org/10.1016/j.bbrep.2015.07.012.

References

[1] A. Enomoto, H. Kimura, A. Chairoungdua, Y. Shigeta, P. Jutabha, S.H. Cha, M. Hosoyamada, M. Takeda, T. Sekine, T. Igarashi, H. Matsuo, Y. Kikuchi, T. Oda, K. Ichida, T. Hosoya, K. Shimokata, T. Niwa, Y. Kanai, H. Endou, Molecular identification of a renal urate anion exchanger that regulates blood urate levels, Nature 417 (2002) 447–452.

[2] K. Mori, Y. Ogawa, K. Ebihara, T. Aoki, N. Tamura, A. Sugawara, T. Kuwahara, S. Ozaki, M. Mukoyama, K. Tashiro, Kidney-specific expression of a novel mouse organic cation transporter-like protein, FEBS Letters 417 (1997) 371–374.

[3] S. Watanabe, D.-H. Kang, L. Feng, T. Nakagawa, J. Kanellis, H. Lan, M. Mazzali, R. J. Johnson, Uric Acid, Hominoid Evolution, and the Pathogenesis of Salt-Sensitivity, Hypertension %R 10.1161/01.HYP.0000028589.66335.AA 40 (2002) 355–360.

[4] T. Nakagawa, D.-H. Kang, D. Feig, L.G. Sanchez-Lozada, T.R. Srinivas, Y. Sautin, A.A. Ejaz, M. Segal, R.J. Johnson, Unearthing uric acid: An ancient factor with recently found significance in renal and cardiovascular disease, Kidney Int 69 (2006) 1722–1725.

[5] D.I. Feig, M. Mazzali, D.-H. Kang, T. Nakagawa, K. Price, J. Kannelis, R.J. Johnson, Serum Uric Acid, A Risk Factor and a Target for Treatment? J Am Soc Nephrol 17 (2006) S69–S73.

[6] M. Kolz, T. Johnson, S. Sanna, A. Teumer, V. Vitart, M. Perola, M. Mangino, E. Albrecht, C. Wallace, M. Farrall, A. Johansson, D.R. Nyholt, Y. Aulchenko, J. S. Beckmann, S. Bergmann, M. Bochud, M. Brown, H. Campbell, J. Connell, A. Dominiczak, G. Homuth, C. Lamina, M.I. McCarthy, T. Meitinger, V. Mooser, P. Munroe, M. Nauck, J. Peden, H. Prokisch, P. Salo, V. Salomaa, N.J. Samani, D. Schlessinger, M. Uda, U. Volker, G. Waeber, D. Waterworth, R. Wang-Sattler, A.F. Wright, J. Adamski, J.B. Whitfield, U. Gyllensten, J.F. Wilson, I. Rudan, P. Pramstaller, H. Watkins, A. Doering, H.E. Wichmann, T.D. Spector, L. Peltonen, H. Volzke, R. Nagaraja, P. Vollenweider, M. Caulfield, T. Illig, C. Gieger, Meta-analysis of 28,141 individuals identifies common variants within five new loci that influence uric acid concentrations, PLoS Genet 5 (2009) e1000504 , doi: 1000510.1001371/journal.pgen.1000504. Epub 1002009 Jun 1000505.

[7] M.J. Caulfield, P.B. Munroe, D. O'Neill, K. Witkowska, F.J. Charchar, M. Doblado, S. Evans, S. Eyheramendy, A. Onipinla, P. Howard, S. Shaw-Hawkins, R. J. Dobson, C. Wallace, S.J. Newhouse, M. Brown, J.M. Connell, A. Dominiczak, M. Farrall, G.M. Lathrop, N.J. Samani, M. Kumari, M. Marmot, E. Brunner, J. Chambers, P. Elliott, J. Kooner, M. Laan, E. Org, G. Veldre, M. Viigimaa, F. P. Cappuccio, C. Ji, R. Iacone, P. Strazzullo, K.H. Moley, C. Cheeseman, SLC2A9 is a high-capacity urate transporter in humans, PLoS Med. 5 (2008) e197 , doi: 110.1371/journal.pmed.0050197.

[8] V. Vitart, I. Rudan, C. Hayward, N.K. Gray, J. Floyd, C.N. Palmer, S.A. Knott, I. Kolcic, O. Polasek, J. Graessler, J.F. Wilson, A. Marinaki, P.L. Riches, X. Shu, B. Janicijevic, N. Smolej-Narancic, B. Gorgoni, J. Morgan, S. Campbell, Z. Biloglav, L. Barac-Lauc, M. Pericic, I.M. Klaric, L. Zgaga, T. Skaric-Juric, S. H. Wild, W.A. Richardson, P. Hohenstein, C.H. Kimber, A. Tenesa, L.A. Donnelly, L.D. Fairbanks, M. Aringer, P.M. McKeigue, S.H. Ralston, A.D. Morris, P. Rudan, N.D. Hastie, H. Campbell, A.F. Wright, SLC2A9 is a newly identified urate transporter influencing serum urate concentration, urate excretion and gout, Nat Genet 40 (2008) 437–442 , doi: 410.1038/ng.1106. Epub 2008 Mar 1039.

[9] A. Doring, C. Gieger, D. Mehta, H. Gohlke, H. Prokisch, S. Coassin, G. Fischer, K. Henke, N. Klopp, F. Kronenberg, B. Paulweber, A. Pfeufer, D. Rosskopf, H. Volzke, T. Illig, T. Meitinger, H.E. Wichmann, C. Meisinger, SLC2A9 influences uric acid concentrations with pronounced sex-specific effects, Nat Genet 40 (2008) 430–436 , doi: 410.1038/ng.1107. Epub 2008 Mar 1039..

[10] M. Lipkowitz, Regulation of Uric Acid Excretion by the Kidney, Current Rheumatology Reports 14 (2012) 179–188.

[11] R.L. George, R.T. Keenan, Genetics of hyperuricemia and gout: implications for the present and future, Curr Rheumatol Rep 15 (2013) 309 , doi: 310.1007/s11926-11012-10309-11928.

[12] A.K. Mandal, D.B. Mount, The Molecular Physiology of Uric Acid Homeostasis, Annual Review of Physiology 77 (2015) 323–345.

[13] A.L. VanWert, M.R. Gionfriddo, D.H. Sweet, Organic anion transporters: discovery, pharmacology, regulation and roles in pathophysiology, Biopharmaceutics & Drug Disposition 31 (2010) 1–71.

[14] S.A. Eraly, K.T. Bush, R.V. Sampogna, V. Bhatnagar, S.K. Nigam, The molecular pharmacology of organic anion transporters: From DNA to FDA? Mol Pharmacol 65 (2004) 479–487.

[15] M. Hosoyamada, K. Ichida, A. Enomoto, T. Hosoya, H. Endou, Function and Localization of Urate Transporter 1 in Mouse Kidney, J Am Soc Nephrol 15 (2004) 261–268.

[16] S.A. Eraly, B.A. Hamilton, S.K. Nigam, Organic anion and cation transporters occur in pairs of similar and similarly expressed genes, Biochem Biophys Res Commun 300 (2003) 333–342.

[17] S.A. Eraly*, V. Vallon*, T. Rieg, J.A. Gangoiti, W.R. Wikoff, G. Siuzdak, B. A. Barshop, S.K. Nigam, Multiple organic anion transporters contribute to net renal excretion of uric acid, Physiol Genomics 33 (2008) 180–192.

[18] S.Y. Ahn, N. Jamshidi, M.L. Mo, W. Wu, S.A. Eraly, A. Dnyanmote, K.T. Bush, T. F. Gallegos, D.H. Sweet, B.O. Palsson, S.K. Nigam, Linkage of organic anion transporter-1 to metabolic pathways through integrated "omics"-driven network and functional analysis, J Biol Chem 286 (2011) 31522–31531 , doi: 31510.31074/jbc.M31111.272534. Epub 272011 Jul 272512.

[19] W. Wu, N. Jamshidi, S.A. Eraly, H.C. Liu, K.T. Bush, B.O. Palsson, S.K. Nigam, Multispecific Drug Transporter Slc22a8 (Oat3) Regulates Multiple Metabolic and Signaling Pathways, Drug Metabolism and Disposition 41 (2013) 1825–1834.

[20] S.A. Eraly, J.C. Monte, S.K. Nigam, Novel slc22 transporter homologs in fly, worm, and human clarify the phylogeny of organic anion and cation transporters, Physiol. Genomics 18 (2004) 12–24.

[21] S.A. Eraly, Striking Differences between Knockout and Wild-Type Mice in Global Gene Expression Variability, PLoS One 9 (2014) e97734 , doi: 97710.91371/journal.pone.0097734. eCollection 0092014.

[22] S.Y. Ahn, S.A. Eraly, I. Tsigelny, S.K. Nigam, Interaction of organic cations with organic anion transporters, J Biol Chem 284 (2009) 31422–31430.

[23] V. Vallon*, S.A. Eraly*, W.R. Wikoff, T. Rieg, G. Kaler, D.M. Truong, S.-Y. Ahn, N. R. Mahapatra, S.K. Mahata, J.A. Gangoiti, W. Wu, B.A. Barshop, G. Siuzdak, S. K. Nigam, Organic anion transporter 3 contributes to the regulation of blood pressure, J Am Soc Nephrol 19 (2008) 1732–1740.

[24] A. Komatsuda, K. Iwamoto, H. Wakui, K. Sawada, A. Yamaguchi, Analysis of mutations in the urate transporter 1 (URAT1) gene of Japanese patients with hypouricemia in northern Japan and review of the literature, Ren Fail. 28 (2006) 223–227.

[25] D. Dinour, A. Bahn, L. Ganon, R. Ron, O. Geifman-Holtzman, A. Knecht, U. Gafter, R. Rachamimov, B.-A. Sela, G. Burckhardt, E.J. Holtzman, URAT1 mutations cause renal hypouricemia type 1 in Iraqi Jews, Nephrology Dialysis Transplantation 26 (2011) 2175–2181.

[26] V. Tasic, A.M. Hynes, K. Kitamura, H.I. Cheong, V.J. Lozanovski, Z. Gucev, P. Jutabha, N. Anzai, J.A. Sayer, Clinical and functional characterization of URAT1 variants, PLoS One 6 (2011) e28641 , doi: 28610.21371/journal.pone.0028641. Epub 0022011 Dec 0028616.

[27] B. Stiburkova, I. Sebesta, K. Ichida, M. Nakamura, H. Hulkova, V. Krylov, L. Kryspinova, H. Jahnova, Novel allelic variants and evidence for a prevalent mutation in URAT1 causing renal hypouricemia: biochemical, genetics and functional analysis, Eur J Hum Genet 21 (2013) 1067–1073.

[28] S. Sugihara, I. Hisatome, M. Kuwabara, K. Niwa, N. Maharani, M. Kato, K. Ogino, T. Hamada, H. Ninomiya, Y. Higashi, K. Ichida, K. Yamamoto, Depletion of Uric Acid Due to SLC22A12 (URAT1) Loss-of-Function Mutation Causes Endothelial Dysfunction in Hypouricemia, Circ J 79 (2015) 1125–1132 , doi: 1110.1253/circj.CJ-1114-1267. Epub 2015 Feb 1123.

[29] A.F. Wright, I. Rudan, N.D. Hastie, H. Campbell, A''complexity' of urate transporters, Kidney Int 78 (2010) 446–452 , doi: 410.1038/ki.2010.1206. Epub 2010

Jul 1037.
[30] H.K. Choi, Y. Zhu, D.B. Mount, Genetics of gout, Curr Opin Rheumatol. 22 (2010) 144–151 , doi: 110.1097/BOR.1090b1013e32833645e32833648.
[31] A. Varki, H.H. Freeze, A.E. Manzi, Overview of glycoconjugate analysis, Curr Protoc Protein Sci, Chapter (2009), http://dx.doi.org/10.1002/0471140864.ps0471141201s0471140857, Unit 12.11 12.11.11-18.
[32] A. Varki, Richard D. Cummings, Jeffrey D. Esko, Hudson H. Freeze, Pamela Stanley, Carolyn R Bertozzi, Gerald W Hart, M.E. Etzler, Essentials of Glycobiology, 2nd edition, Cold Spring Harbor Laboratory Press, NY, 2009.
[33] S.K. Nigam, K.T. Bush, Growth factor-heparan sulfate "switches" regulating stages of branching morphogenesis, Pediatr Nephrol 29 (2014) 727–735 , doi: 710.1007/s00467-00013-02725-z. Epub 02014 Feb 00462.
[34] D.G. Hackam, S.S. Anand, Emerging risk factors for atherosclerotic vascular disease: a critical review of the evidence, Jama 290 (2003) 932–940.
[35] S.J. Hayflick, Defective pantothenate metabolism and neurodegeneration, Biochem Soc Trans. 42 (2014) 1063–1068 , doi: 1010.1042/BST20140098.
[36] F.L. Theodoulou, O.C. Sibon, S. Jackowski, I. Gout, Coenzyme A and its derivatives: renaissance of a textbook classic, Biochem Soc Trans. 42 (2014) 1025–1032 , doi: 1010.1042/BST20140176.
[37] B. Srinivasan, O.C. Sibon, Coenzyme A, more than"just' a metabolic cofactor, Biochem Soc Trans. 42 (2014) 1075–1079 , doi: 1010.1042/BST20140125.
[38] S.K. Nigam, What do drug transporters really do? Nat Rev Drug Discov 14 (2015) 29–44.
[39] S.K. Nigam, K.T. Bush, G. Martovetsky, S.-Y. Ahn, H.C. Liu, E. Richard, V. Bhatnagar, W. Wu, The Organic Anion Transporter (OAT) Family: A Systems Biology, Perspective, American Physiological Society, 2015.
[40] S.Y. Ahn, S.K. Nigam, Toward a systems level understanding of organic anion and other multispecific drug transporters: a remote sensing and signaling hypothesis, Mol Pharmacol 76 (2009) 481–490 , doi: 410.1124/mol.1109.056564. Epub 052009 Jun 056510.
[41] R.H. Waterston, K. Lindblad-Toh, E. Birney, J. Rogers, J.F. Abril, P. Agarwal, R. Agarwala, R. Ainscough, M. Alexandersson, P. An, S.E. Antonarakis, J. Attwood, R. Baertsch, J. Bailey, K. Barlow, S. Beck, E. Berry, B. Birren, T. Bloom, P. Bork, M. Botcherby, N. Bray, M.R. Brent, D.G. Brown, S.D. Brown, C. Bult, J. Burton, J. Butler, R.D. Campbell, P. Carninci, S. Cawley, F. Chiaromonte, A. T. Chinwalla, D.M. Church, M. Clamp, C. Clee, F.S. Collins, L.L. Cook, R.R. Copley, A. Coulson, O. Couronne, J. Cuff, V. Curwen, T. Cutts, M. Daly, R. David, J. Davies, K.D. Delehaunty, J. Deri, E.T. Dermitzakis, C. Dewey, N.J. Dickens, M. Diekhans, S. Dodge, I. Dubchak, D.M. Dunn, S.R. Eddy, L. Elnitski, R.D. Emes, P. Eswara, E. Eyras, A. Felsenfeld, G.A. Fewell, P. Flicek, K. Foley, W.N. Frankel, L.A. Fulton, R.S. Fulton, T.S. Furey, D. Gage, R.A. Gibbs, G. Glusman, S. Gnerre, N. Goldman, L. Goodstadt, D. Grafham, T.A. Graves, E.D. Green, S. Gregory, R. Guigo, M. Guyer, R.C. Hardison, D. Haussler, Y. Hayashizaki, L.W. Hillier, A. Hinrichs, W. Hlavina, T. Holzer, F. Hsu, A. Hua, T. Hubbard, A. Hunt, I. Jackson, D.B. Jaffe, L.S. Johnson, M. Jones, T.A. Jones, A. Joy, M. Kamal, E.K. Karlsson, et al., Initial sequencing and comparative analysis of the mouse genome, Nature., 420, (2002) 520–562.